INTERNAL-EXTERNAL FLOW INTEGRATION FOR A THIN EJECTOR-FLAPPED WING SECTION

Henry W. Woolard

Flight Control Division
Air Force Flight Dynamics Laboratory
Wright-Patterson Air Force Base

SUMMARY

Some results from a thin-airfoil theory of an ejector-flapped wing section are reviewed briefly with particular attention given to the global matching of the external airfoil flow with the ejector internal flow and the overall ejector-flapped wing-section aerodynamic performance.

INTRODUCTION

Within the last two decades, considerable numbers of high-lift concepts for V/STOL aircraft have been proposed. One among these is the ejector-flapped wing (fig. 1) also known as the augmentor wing, the ejector wing, the augmented jet-flap wing, etc. The ejector-flapped wing operates on a principle similar to the ordinary jet-flapped wing in that use is made of a trailing jet sheet to increase the circulation about the wing itself. It differs from the jet-flapped wing in the presence of ejector air intakes and the existence of an augmented trailing-edge momentum flux resulting from the ejector action. Since the augmented trailing-edge momentum flux is an internal-flow phenomenon, the basic difference in the external aerodynamics of the two systems is due to the air-intake flows. The intake flows behave as sink flows and are not accounted for in the usual jet-flap theory (refs. 1 and 2).

Woolard, in reference 3, has performed a theoretical analysis of an ejector-flapped wing section based on a small-perturbation thin-airfoil mathematical model which takes into account the intake sink flows. Although much of the emphasis of reference 3 was on the thin-airfoil modeling of the external flow, the paper was also concerned with the global matching of the airfoil external flow with the ejector internal flow and the overall ejector-flapped wing-section aerodynamic performance. Since the theme of this workshop is thrust-augmenting ejectors, the principal emphasis in this overview of reference 3 will be on global matching and overall aerodynamic performance.

This paper is intended to be only a brief overview of reference 3. Greater detail may be found in the original document.

SYMBOLS

A	cross-sectional area
b_f	ejector-flap span
c	airfoil chord
c_f	flap chord
c_j	primary-jet installed momentum coefficient, $\rho U_j^2 \bar{h}_j/q_\infty c$
$\hat{c}_j$	primary-jet uninstalled momentum coefficient, $\rho \hat{U}_j^2 \bar{h}_j/q_\infty c$
c_j^*	primary-jet test momentum coefficient, $\rho U_j \bar{h}_j \hat{U}_j/q_\infty c$
c_J	ejector exit-flow momentum coefficient, $\rho U_E^2 h_E/q_\infty c$
c_ℓ	lift coefficient
c_{m_o}	airfoil nose-up pitching-moment coefficient about the leading edge
c_Q	thin airfoil suction coefficient, $Q/U_\infty c$
c_Q	ejector net suction coefficient, $(U_s - U_\infty)\bar{h}_s/U_\infty c$
$\check{c}_Q$	ejector gross suction coefficient, $U_s \bar{h}_s/U_\infty c$; $(\check{c}_q = c_q + \bar{h}_s/c)$
c_T	ejector net-thrust coefficient, $(\rho U_E^2 h_E - \rho U_s U_\infty \bar{h}_s/q_\infty c)$
$\hat{c}_t$	primary-jet uninstalled net-thrust coefficient, $\rho \hat{U}_j (\hat{U}_j - U_\infty)\bar{h}_j/q_\infty c$
h_e, h_E	heights at ejector diffuser inlet and exit, respectively
$\bar{h}_j$	mean height of ejector primary-jet nozzle, A_j/b_f
$\bar{h}_s$	mean height of ejector secondary flow passage at primary-jet A_s/b_f
p	static pressure
P	total pressure
q_∞	free-stream dynamic pressure, $(\rho/2)U_\infty^2$
Q	two-dimensional ideal-flow sink strength
U	mean local axial velocity within the ejector (except U_∞)
$\hat{U}_j$	primary-jet uninstalled isentropic velocity, $[(2/\rho)(P_j - p_\infty)]^{1/2}$

$\bar{U}_x$ $U_x/\hat{U}_j$, where x = j, s, E, etc.

U_∞ free-stream velocity

$\bar{U}_\infty$ forward-speed parameter, $U_\infty/\hat{U}_j$

x,y rectangular coordinates, see figure 2

x_s chordwise location of sink on airfoil of unit chord

α angle of attack

δ_f trailing-edge flap deflection angle, positive for trailing edge down

ρ density

σ $\sigma = 1$ for an upper-surface sink, $\sigma = -1$ for a lower-surface sink

Ω_D ejector diffuser area ratio, A_E/A_e

Ω_j ejector injection area ratio, A_s/A_j

$( )_D$ denotes the diffuser

$( )_e$ ejector station e, see figure 6

$( )_E$ ejector station E, see figure 6

$( )_{EF}$ denotes an ejector-flapped wing

$( )_f$ denotes the trailing-edge flap

$( )_j$ denotes station j and the ejector primary jet, see figure 6

$( )_{JF}$ denotes a jet-augmented-flapped wing

$( )_s$ denotes the ejector secondary flow (except x_s)

$( )_\infty$ denotes a free-stream quantity

$\hat{(\ )}$ denotes quantities associated with isentropic flow from P_j to p_∞

$\bar{(\ )}$ denotes a velocity normalized by dividing by $\hat{U}_j$

$\overline{(\ )}$ denotes a mean quantity

DISCUSSION

The External Aerodynamics

A thin-airfoil representation of an ejector-flapped wing section having an upper intake only is shown in figure 2. The main airfoil and flap are approximated by straight lines, the ejector net intake flow by a surface sink[1] (not necessarily at the flap knee, but usually taken there), and the actual jet sheet of finite thickness by an infinitesimally thin sheet having a finite internal momentum. In this approximation the ejector intake and exhaust openings are required to be small relative to the airfoil chord. The internal and external flow fields are not required to match in fine detail at their interface, but the values of the ejector intake net mass flow and ejector exhaust total momentum flux must match those used in external flow aerodynamics.

Although figure 2 is illustrative of the modeling for an ejector-flapped wing section with an upper intake only, the fundamental solution obtained in reference 3 is valid for any sink location on the wing upper or lower surface. Since the governing equations are linear for the small perturbation analysis of reference 3, solutions and boundary conditions are additive and a solution for an ejector-flapped wing section having both upper and lower intakes is obtained by adding the appropriate individual solutions for upper and lower surface sink flows.

The flow shown in figure 2 consists of three additive components as illustrated on the left-hand side of figure 3. These are: 1) the flow about a flat plate at angle of attack with trailing-edge tangential (regular) blowing; 2) the flow about a flapped airfoil at zero angle of attack with regular blowing; 3) the flow about a flat-plate suction airfoil at zero angle of attack with regular blowing, as shown in the bottom left-hand illustration of figure 3. Shown for comparison on the right-hand side of figure 3 is an idealized representation of a real-flow ejector-flapped wing having an ejector without a diffuser. Spense in references 1 and 2, respectively, has solved the aforementioned flow component cases 1 and 2. The solution for the flow about the flat-plate suction airfoil shown in figures 3 and 4 is given by Woolard in reference 3.

Although the external flow analysis of Woolard yields other aerodynamic details, only the lift and pitching moment coefficients will be discussed here. These characteristics are given by

$$c_\ell = (\partial c_\ell/\partial\alpha)\alpha + (\partial c_\ell/\partial\delta_f)\delta_f + (\partial c_\ell/\partial c_Q)c_Q \qquad (1)$$

$$c_{m_o} = (\partial c_{m_o}/\partial\alpha)\alpha + (\partial c_{m_o}/\partial\delta_f)\delta_f + (\partial c_{m_o}/\partial c_Q)c_Q \qquad (2)$$

where the component terms on the right-hand sides of equations (1) and (2) are the contributions of the various component flows illustrated on the left-hand

[1]A sink for which the flow enters a point from only one side of a surface.

side of figure 3. All the partial derivatives in equations (1) and (2) are functions of the jet-momentum coefficient, c_J. The derivatives with respect to δ_f and c_Q are also functions respectively of the flap chord to airfoil chord ratio and the sink (intake) chordwise location. It is the third term on the right-hand side of equations (1) and (2) that involves matching of the ejector flow characteristics, since for a given ejector geometry, ejector primary air-supply pressure ratio, and ejector forward speed, a specific relation exists for c_Q/c_j.

Curves showing $(\partial c_\ell/\partial c_Q)/\sigma$ and $(\partial c_{m_o}/\partial c_Q)/\sigma$ as a function of c_J for several sink locations are presented in figure 5. The parameter σ employed in the figure provides for the placement of a sink (intake) on the upper or lower surface or both. For an upper surface sink, $\sigma = -1$; while for a lower surface sink, $\sigma = -1$. It is seen in figure 5, that for a sink on the upper surface only, the sink effect alone (i.e., $c_J = 0$) contributes an incremental increase to the lift coefficient that becomes larger as the sink approaches the trailing edge. It is also seen that the interference effect of the jet sheet ($c_J \neq 0$) decreases the lift coefficient and increases the nose-up pitching moment.

The Suction Coefficient

The discussion thus far has been concerned with a thin-airfoil approximation in which the real airfoil and the ejector shroud (or shrouds) are taken to lie on a single skeletal line. A real ejector-flapped wing, however, has a finite-height intake (or intakes) and a question arises regarding the application of a limiting process in which the intake height is reduced to zero in a manner such that the thin-airfoil aerodynamics most appropriately represents the real-airfoil aerodynamics. Since the thin-airfoil approximation is an imperfect representation of the real flow, there cannot be a one-to-one correspondence between the real and theoretical flows and a decision must be made regarding which properties are to be matched in a thin-airfoil representation. Certainly the lift coefficient is an important quantity to be conserved. The thrust coefficient is of lesser importance in the thin-airfoil representation since it is easily determined from considerations of conservation of global momentum applied directly to the real flow. As an intermediate step to taking the limiting process, consider the "idealized real wing" shown in figure 6 representing a real ejector-flapped wing (with upper shroud only) at zero angle of attack and zero flap deflection. In this representation, the main airfoil and the shroud are of infinitesimal thickness, but the total airfoil is not a thin airfoil because of the small, but finite, intake height (exaggerated in the figure for clarity). For an arbitrary intake flow in figure 5 there is no formal procedure for applying a limiting process in which the lift coefficient is held constant. However, as will be shown subsequently, the appropriate limit can be obtained by inductive reasoning. On the other hand, the limit in which the intake mass flow is held constant while the intake height is reduced to zero is easily implemented by simply taking the theoretical sink mass flow equal to the gross intake mass flow of the real wing. In this case, the suction coefficient used in the

theoretical relations is the ejector gross suction coefficient, $\check{c}_Q$. Use of the gross suction coefficient is suggested by Chan (ref. 4) and Lopez (ref. 5). On the bases of the argument which follows and a comparison with other work, the present author maintains that the ejector net suction coefficient, c_Q, is the correct suction coefficient to use in the thin airfoil representation.

For the purposes of the present argument, the idealized real flow in figure 6 is taken to be the real flow since the intake has a finite height. Now consider a flow in which the intake capture streamline is parallel to the main airfoil as shown by the dashed line a'b in figure 6. For this situation, $c_Q = 0$ and $\check{c}_Q = h_s/c$. Since in this case all the streamlines of the idealized real flow are parallel there is no lift (or moment) on the real wing, hence the thin-airfoil theory should yield zero lift and moment. Use of the ejector net suction coefficient, $c_Q = 0$, in the thin-airfoil results of figure 5 for this case, yields the proper zero lift and moment; use of the ejector gross suction coefficient, $\check{c}_Q = h_s/c$, however, yields incorrect non-zero values for the lift and moment. It follows that the thin-airfoil lift and moment coefficients based on c_Q will be in error also for an arbitrary intake mass flow ($c_Q \neq h_s/c$).

Although matching of the thin-airfoil and real flows by means of the net suction coefficient yields the proper lift and pitching-moment coefficients in the thin-airfoil approximation, it fails to give the correct thrust coefficient. This latter property is easily obtained from the real flow as $c_T = c_J - 2\,(c_Q + \bar{h}_s/c)$. Inconsistencies of this type frequently occur in approximate representations of complicated flows, and generally are tolerated for the purposes of obtaining an engineering estimate of the problem being solved.

Although it is believed that the foregoing argument demonstrates that the ejector net suction coefficient, c_Q, is the proper coefficient to use in the thin-airfoil approximation, additional justification is provided by the following comparison with the work of Sidor (ref. 6).

Sidor has performed an analysis and digital-computer computation for the flow situation illustrated in figure 7. Sidor employs distributed vortices over the main airfoil, over the upper and lower ejector shroud surfaces, and over the upper and lower interfaces of the jet sheet. The flow momentum imparted by the ejector is represented by an actuator disk located at the aft end of the ejector shrouds as indicated in figure 7. For $\alpha = \delta_f = 0$, Sidors model is analogous to the flow situation of figure 4 and therefore can be used to obtain a rough check of how well the present sink-flow jet-flap model approximates the flow for a finite height shroud, and to provide also some insight regarding the selection of the proper suction coefficient.

For $\alpha = \delta_f = 0$, the variation of the lift coefficient with the jet-momentum coefficient, c_J, for the actuator-disk flow model (taken from ref. 6) is shown in figure 8. Also shown in figure 8 are the lift coefficient curves for the sink-flow jet-flap model based on the net and gross intake suction

coefficients corresponding to the relationship[2] between c_Q and c_j for the actuator disk. Since the curve based on the use of the net-suction coefficient agrees much more favorably with the actuator-disk flow model curve, it can be concluded from this agreement and the previously presented argument that the net-suction coefficient, c_Q, is the proper one to use in the present model.

One-Dimensional Ejector-Flow Relations

A schematic representation of an ejector flap is given in figure 9. The ejector internal flow is taken to be incompressible and is analyzed on the basis of assumptions that the flow properties are uniform at any given cross-sectional station and there are no flow losses except those due to mixing. It is recognized that this is an oversimplification for aircraft design purposes. The purpose here, however, is to delineate the general characteristics of the integrated external-internal aerodynamic system and this is best accomplished by keeping the mathematical modeling as simple as possible.

The primary air is injected at station j (see fig. 9), and mixing with the secondary air is assumed to be completed at the end of the constant cross-sectional area region extending between stations j and e. It is assumed also that the static pressures of the primary and secondary streams are equal at the injection station j and that the diffuser-exit static pressure is equal to the free-stream static pressure. In view of the assumption of loss-free flow in the intake, the primary nozzle, and the diffuser, Bernoulli's equation is applicable to these regions.

In the ejector analytics, flow velocities are nondimensionalized by dividing by $\hat{U}_j$, where $\hat{U}_j$ is the velocity attained by the primary nozzle exhausting isentropically to the free-stream static pressure. This velocity is a measure of the primary-air total pressure, the quantity most likely to be held constant during the major portion of a landing or take-off operation.

On the base of the aforementioned assumptions, the governing equations for the ejector internal flow are

$$2\tilde{U}_j^2 - \tilde{U}_s^2(1 - \Omega_j) - \tilde{U}_E^2(1 + \Omega_D^2)(1 + \Omega_j) + \tilde{U}_\infty^2(1 + \Omega_j) = 0 \tag{3}$$

$$\tilde{U}_j + \tilde{U}_s\Omega_j = \tilde{U}_E(1 + \Omega_j)\Omega_D \tag{4}$$

$$\tilde{U}_j^2 = \tilde{U}_s^2 - \tilde{U}_\infty^2 + 1 \tag{5}$$

Equations (3) and (4) are respectively expressions of conservation of momentum and mass between stations j and e in figure 9. These forms of the conservation equations were derived from the basic forms by appropriate use of Bernoulli's equation, continuity, and the previously mentioned assumptions.

[2]For the actuator disk, it is easily shown that the relation between the net-suction coefficient and the jet-momentum coefficient is given by $c_Q = [(h/c)c_J 2]^{1/2} - (h/c)$.

Equation (5) is a consequence of the equality of p_s and p_j and the use of Bernoulli's equation for the primary and secondary flows.

The quantities $\tilde{U}_j$ and $\tilde{U}_E$ may be eliminated from equation (1) through the use of equations (3) and (4), yielding the following quadratic equation in $\tilde{U}_s$?

$$a_o\tilde{U}_s^4 + (b_o + b_2\tilde{U}_\infty^2)\tilde{U}_s^2 + c_o + c_2\tilde{U}_\infty^2 + c_4\tilde{U}_\infty^4 = 0 \tag{6}$$

where

$$a_o = (\Omega_j + 1)^2 [\Omega_j^2 - 2(1 + 2\Omega_D^2)\Omega_j + 1] \tag{7}$$

$$b_o = -4\Omega_D^2\Omega_j^3 + 2(2\Omega_D^4 - 5\Omega_D^2 - 1)\Omega_j^2 + 4(\Omega_D^4 - 2\Omega_D^2)\Omega_j - 2\Omega_D^2 + 2 \tag{8}$$

$$b_2 = -2\Omega_D^2\Omega_j^4 + 4\Omega_D^4\Omega_j^3 + 2(2\Omega_D^4 + 3\Omega_D^2 + 1)\Omega_j^2 + 4\Omega_D^2\Omega_j - 2 \tag{9}$$

$$c_o = [\Omega_D^2 - (1 - 2\Omega_D^2\Omega_j)]^2 \tag{10}$$

$$c_2 = 2(1 + \Omega_D^2\Omega_j^2)[\Omega_D^2 - (1 - 2\Omega_D^2\Omega_j)] \tag{11}$$

$$c_4 = (1 + \Omega_D^2\Omega_j^2)^2 \tag{12}$$

Equation (6) may be solved for $\tilde{U}_s^2$ by the standard quadratic formula. For the sign options preceding the radical, the negative sign must be selected. The numerics are much more convenient, however, if equation (6) is divided through by a_o and then solved by the quadratic formula. In this case, the sign of the radical is given by $(-\text{sgn } a_o)$.

Solution of equation (6) yields $\tilde{U}_s$ as a function of the forward-speed parameter, $\tilde{U}_\infty$, the injection area ratio, Ω_j, and the diffuser area ratio, Ω_D. With $\tilde{U}_s$ known, $\tilde{U}_E$ and $\tilde{U}_j$ can be determined as functions of $\tilde{U}_\infty$, Ω_j, and Ω_D by means of equations (4) and (5). By appropriate substitutions, the ejector coefficients, $\hat{c}_j$, c_j^*, $\hat{c}_t$, c_Q, and c_Q (see symbols) also can be determined as functions of U, Ω_j, Ω_D.

Some selected ejector characteristics as functions of the forward-speed ratio are shown in figures 10 through 12 for a diffuser area ratio of unity. For aircraft high-lift operations, forward-speed ratios in the vicinity of 0.1 may be anticipated. For a primary nozzle speed of 1000 ft/sec, say, this corresponds to a flight speed of 100 ft/sec.

Shown in figure 10 is the exit-momentum ratio $c_J/\hat{c}_j$. This parameter has a value of unity for a jet flap and is a measure of the increase in the exit-momentum coefficient of an ejector flap over that of a jet flap having the same primary-air supply pressure ratio. The parameter, c_J/c_j is important to the lift. It is apparent from the figure that both forward speed and increased injection-area ratio are beneficial to increasing $c_J/\hat{c}_j$. The thrust, however, behaves differently with forward speed and injection-area ratio as may be seen in figure 11. It is seen in this figure that regardless of the injection-area ratio the thrust augmentation decreases with forward speed, reaching values of less than 1.1 for speed ratios in excess of 0.3. At small forward-speed ratios

the thrust augmentation increases with increasing injection-area ratio while at the high ratios the opposite occurs. In the region of potential interest for high-lift systems ($\hat{U}_\infty/U_j = 0.1$) the injection-area ratio has little effect except at very low area ratios.

Finally, the behavior of the net suction coefficient with forward speed ratio is shown in figure 12 which indicates that for a constant area ratio, A_s/A_j, the suction coefficient reaches a maximum value at a particular forward-speed ratio. The maximum suction coefficient and the corresponding speed ratio are seen to be a function of the injection-area ratio, although at the higher area ratios the variation of the maximum with speed ratio is slight. For area ratios of interest for high-lift systems ($A_s/A_j \cong 10$) the maximum coefficients occur at forward-speed ratios typical of high-lift systems. It is seen also from figure 12 that for the maximum suction coefficients and a c_J of unity, c_Q and δ_f are of the same order of magnitude for flap angles of approximately five degrees. Hence in this regime, for small flap-chord to airfoil-chord ratios at which $(\partial c_\ell/\partial c_Q)$ and $(\partial c_\ell/\partial \delta_f)$ are of approximately the same order of magnitude, the suction and flap lift contributions are also of approximately the same order of magnitude.

Relative Lift Performance

The lift performance of an ejector-flapped wing relative to that of a wing with a jet-augmented flap, based on the relations given in this paper, is shown in figure 13 for typical values of the pertinent parameters. It can be seen in the figure that for forward-speed ratios below 0.3 the ejector-flap lift is substantially superior and continues to increase in superiority as the forward speed is reduced. The superiority also increases with increasing ejector size as indicated by the gains accompanying the change in the relative nozzle height from 0.005 to 0.010. The lift superiority of the ejector-flapped wing also increases with decreasing flap deflection. As may be seen in figure 14, this effect is because the relative suction contribution to the lift of the ejector-flapped wing is larger at lower flap angles.

CONCLUDING REMARKS

On the basis of simple mathematical models of the external and internal flows, an integrated theoretical analysis of the aerodynamics of an ejector-flapped wing was developed in reference 3. The external aerodynamics was systemized for ease of application in the aforementioned reference by inclusion of a table of Fourier coefficients. The incompressible, idealized, forward-speed ejector-flow equations from reference 3 have been presented in this paper. The normalized form used for these equations is believed to be the most appropriate for interfacing with the external aerodynamics. Some parametric curves of ejector forward-speed characteristics have been also presented. Although forward-speed effects on exit momentum and net thrust of ejectors are generally well-known, it is believed to have been worthwhile to reemphasize these and cast them in a form appropriate for interfacing with the external aerodynamics. The delineation of the suction-flow coefficient

characteristics is believed to be new or at least relatively unfamiliar. The idealized lift performance of an ejector-flapped wing relative to a jet-augmented-flapped wing has been compared and the ejector-flapped wing was found to be substantially superior at low forward-speed ratios. Finally, it was determined that the suction effect on the lift is most significant at low flap angles.

Despite the idealized character of the flow model, it is believed that it adequately delineates the important trends. Because of its relative simplicity, it is easily amenable to empirical modification for use as a preliminary design tool.

REFERENCES

1. Spence, D. A.: The Lift Coefficient of a Thin Jet-Flapped Wing. Proceedings of the Royal Society of London, ser. A, vol. 238, no. 1212, Dec. 1956, pp. 46-48.

2. Spence, D. A.: The Lift of a Thin Aerofoil with a Jet-Augmented Flap. The Aeronautical Quarterly, vol. 9, pt. 3, Aug. 1958, pp. 287-299.

3. Woolard, Henry W.: Thin-Airfoil Theory of an Ejector-Flapped Wing Section. Journal of Aircraft, vol. 12, no. 1, Jan. 1975; also AIAA Paper 74-187.

4. Chan, Y. Y.: Lift Induced by Suction Flaps on Augmentor Wings. Canadian Aeronautics and Space Institute Transactions, vol. 3, no. 2, Sept. 1970, pp. 107-110.

5. Lopez, M. L.; and Wasson, N. F.: A Theoretical Method for Calculating the Aerodynamic Characteristics of Arbitrary Ejector-Jet-Flapped Wings. Air Force Systems Command, AFFDL-TR-74-72, June 1944, (AD-A-002319).

6. Sidor, Laurent B.: An Investigation of the Ejector-Powered Jet-Flap. Thesis for the Degree of Aeronautical Engineer, Calif. Inst. of Technology, 1974. Also published in "Theoretical and Experimental Study on the Ejector Augmented Jet Flap" by H. J. Stewart. NASA CR-136749, Aug. 1974 (N75-17296#).

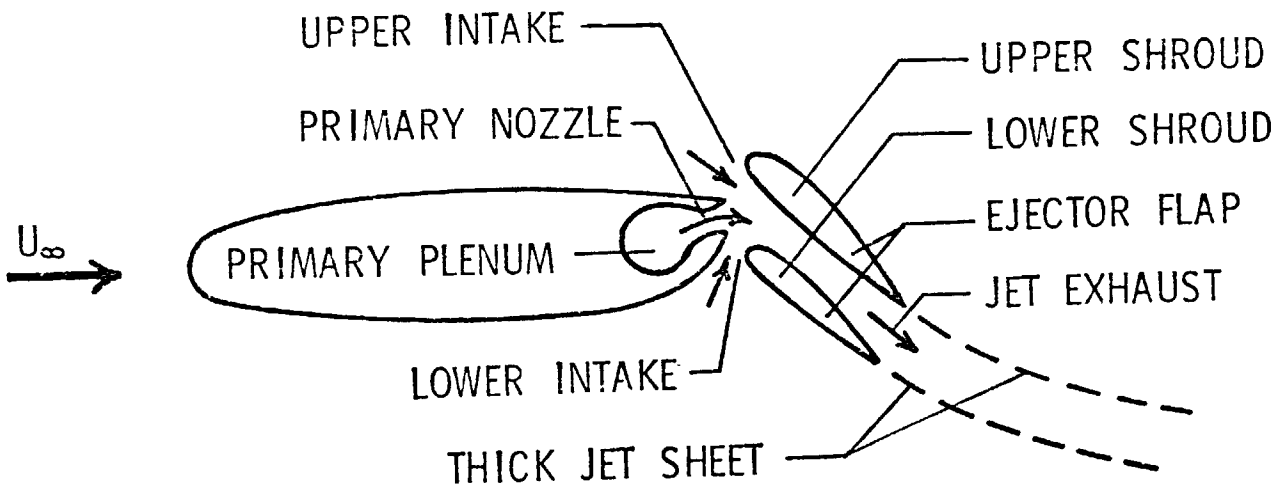

Figure 1.- Ejector-flapped wing section.

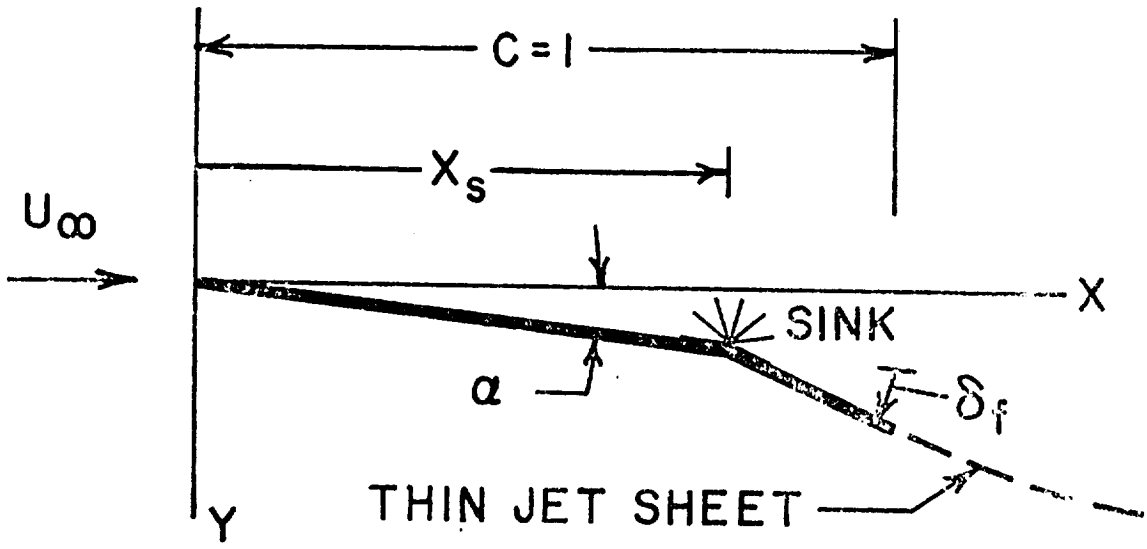

Figure 2.- Thin-airfoil representation of an ejector-flapped wing with an upper-surface intake only.

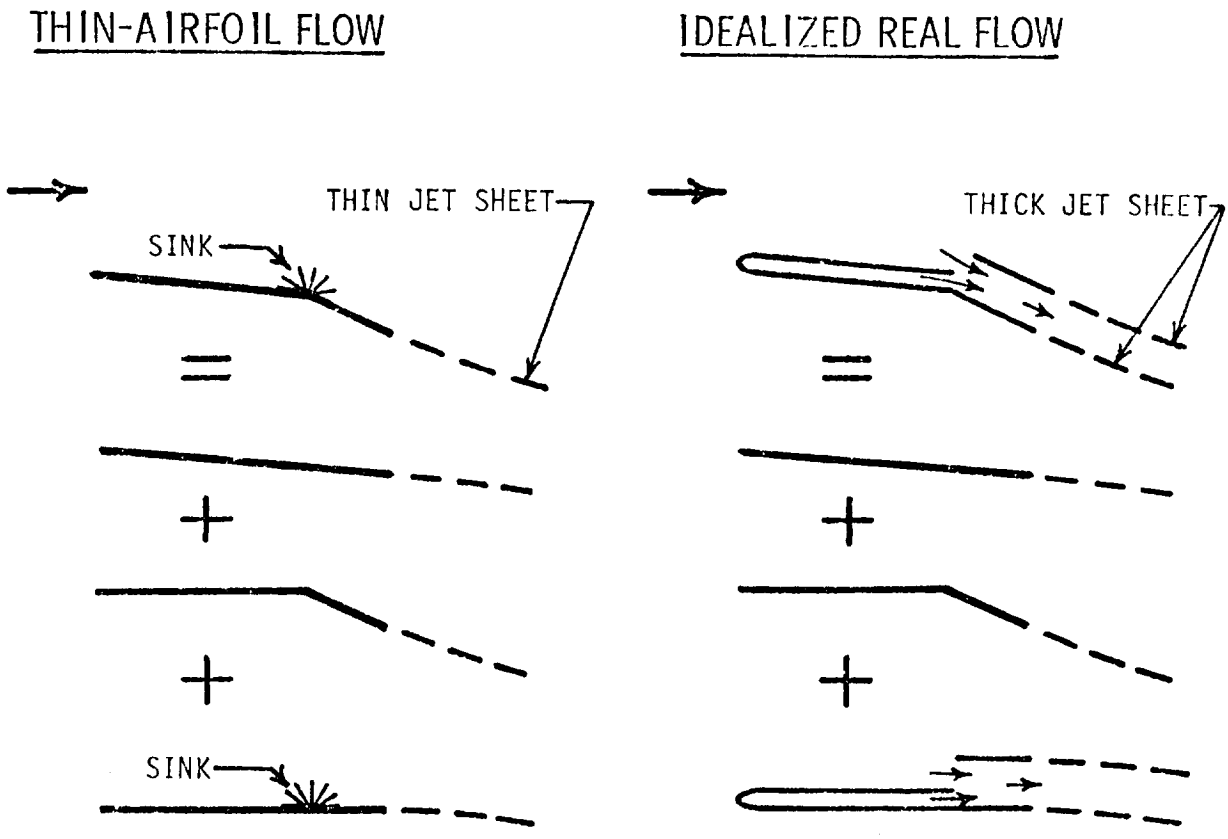

Figure 3.- Illustration of superposition principle.

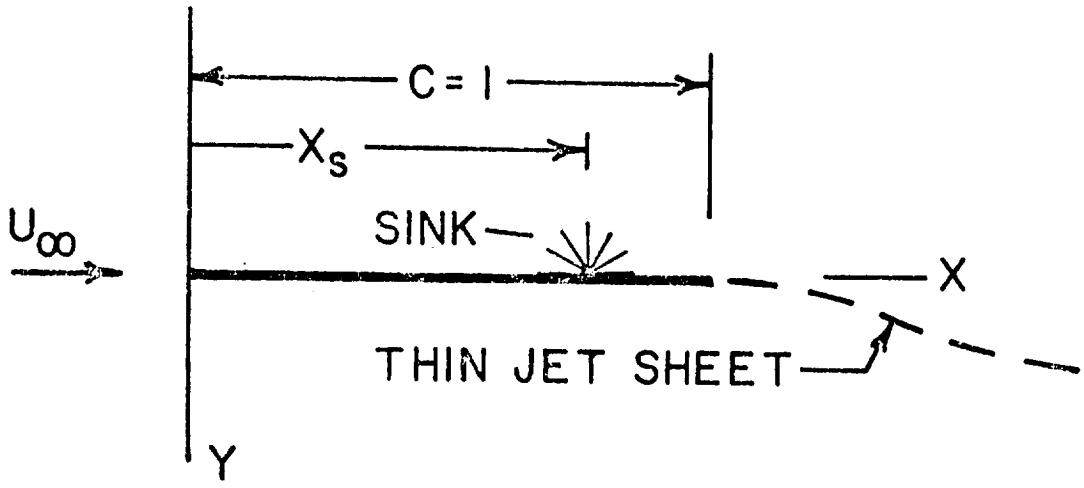

Figure 4.- Flat-plate suction airfoil with trailing-edge regular blowing.

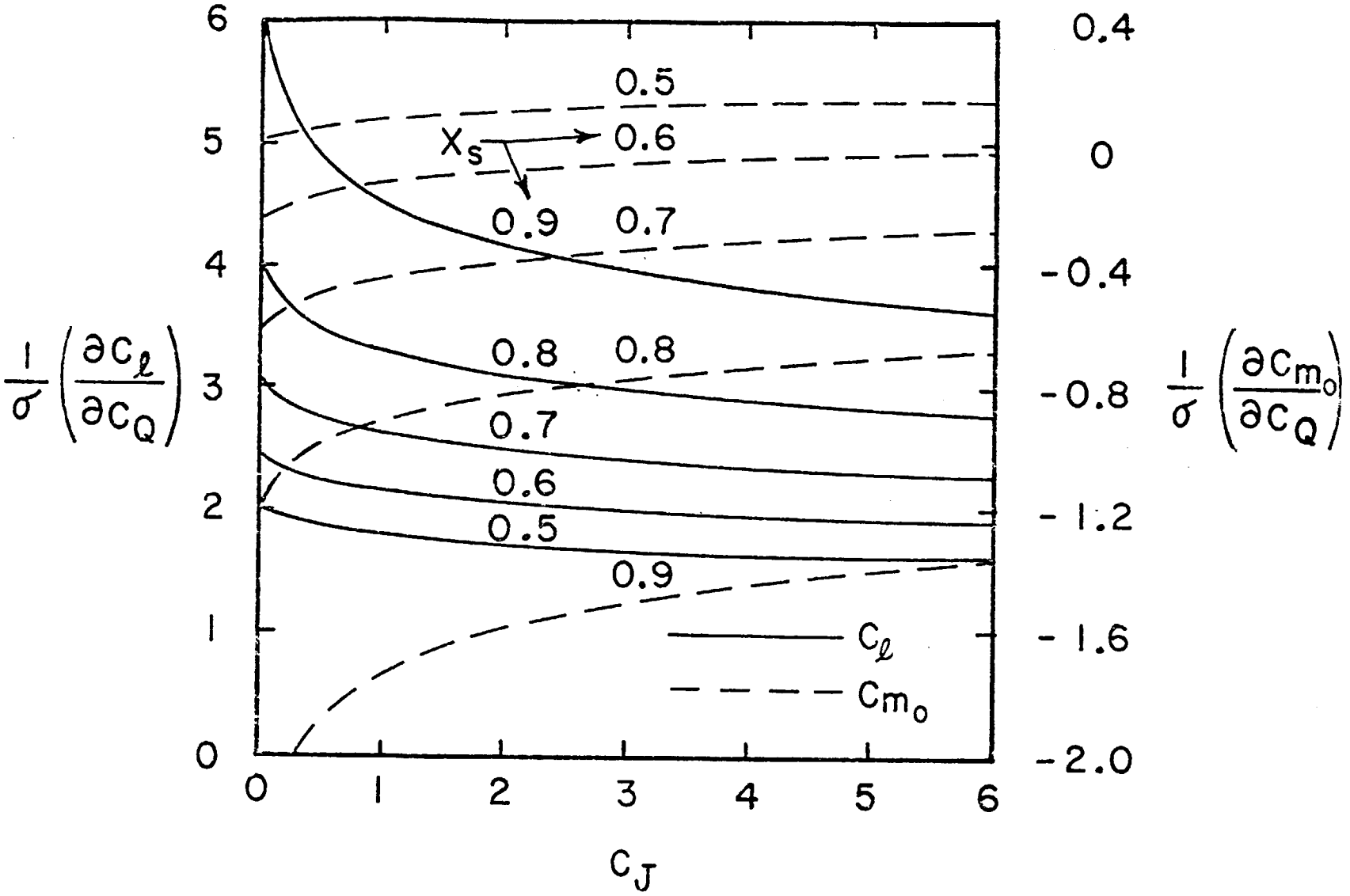

Figure 5.- Lift and pitching-moment characteristics of a flat-plate suction airfoil with trailing-edge regular blowing.

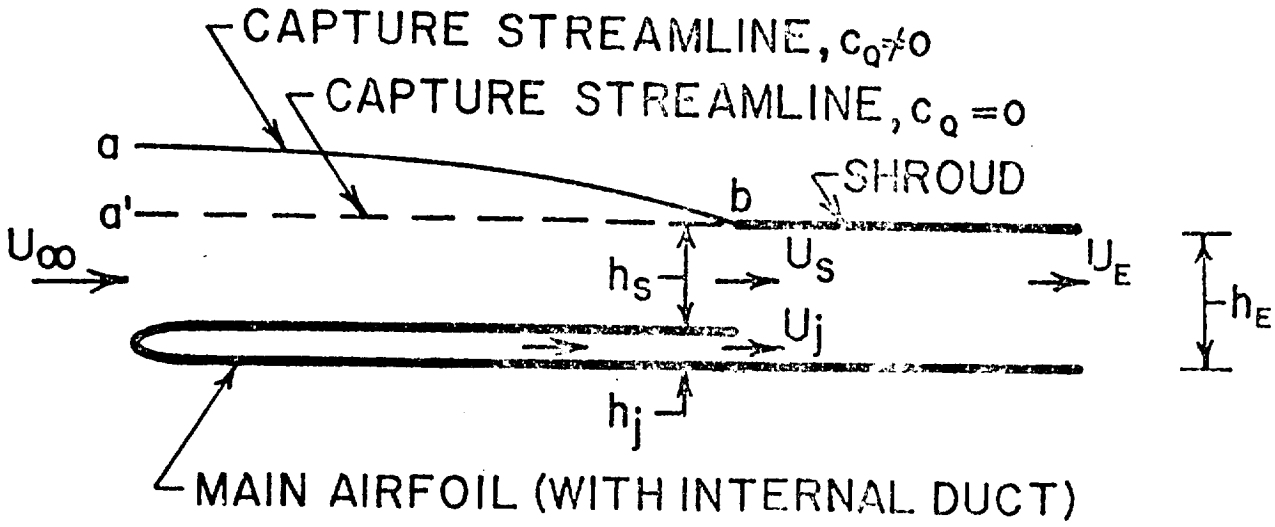

Figure 6.- Idealized ejector-flapped wing section defining $c_Q = 0$.

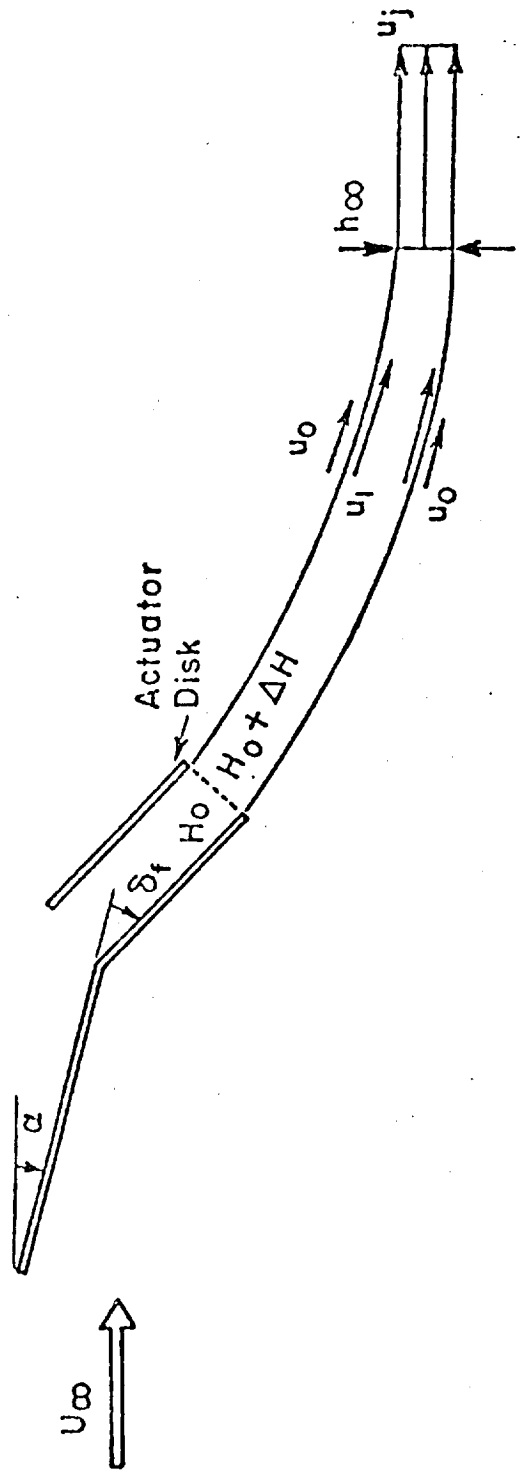

Figure 7.- Galcit actuator-disk flow model.

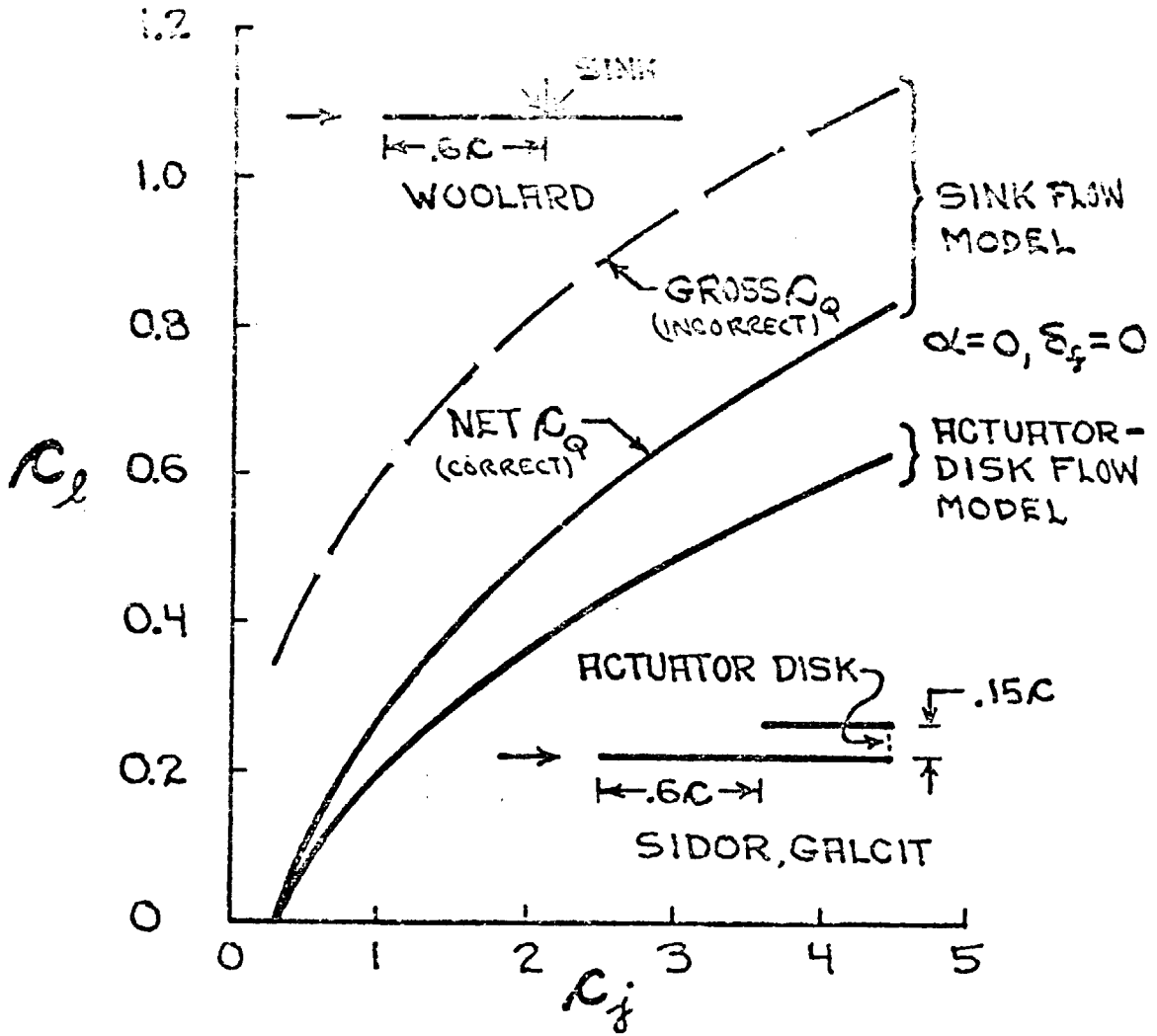

Figure 8.- Comparison of the suction-induced lift coefficients for several flow models.

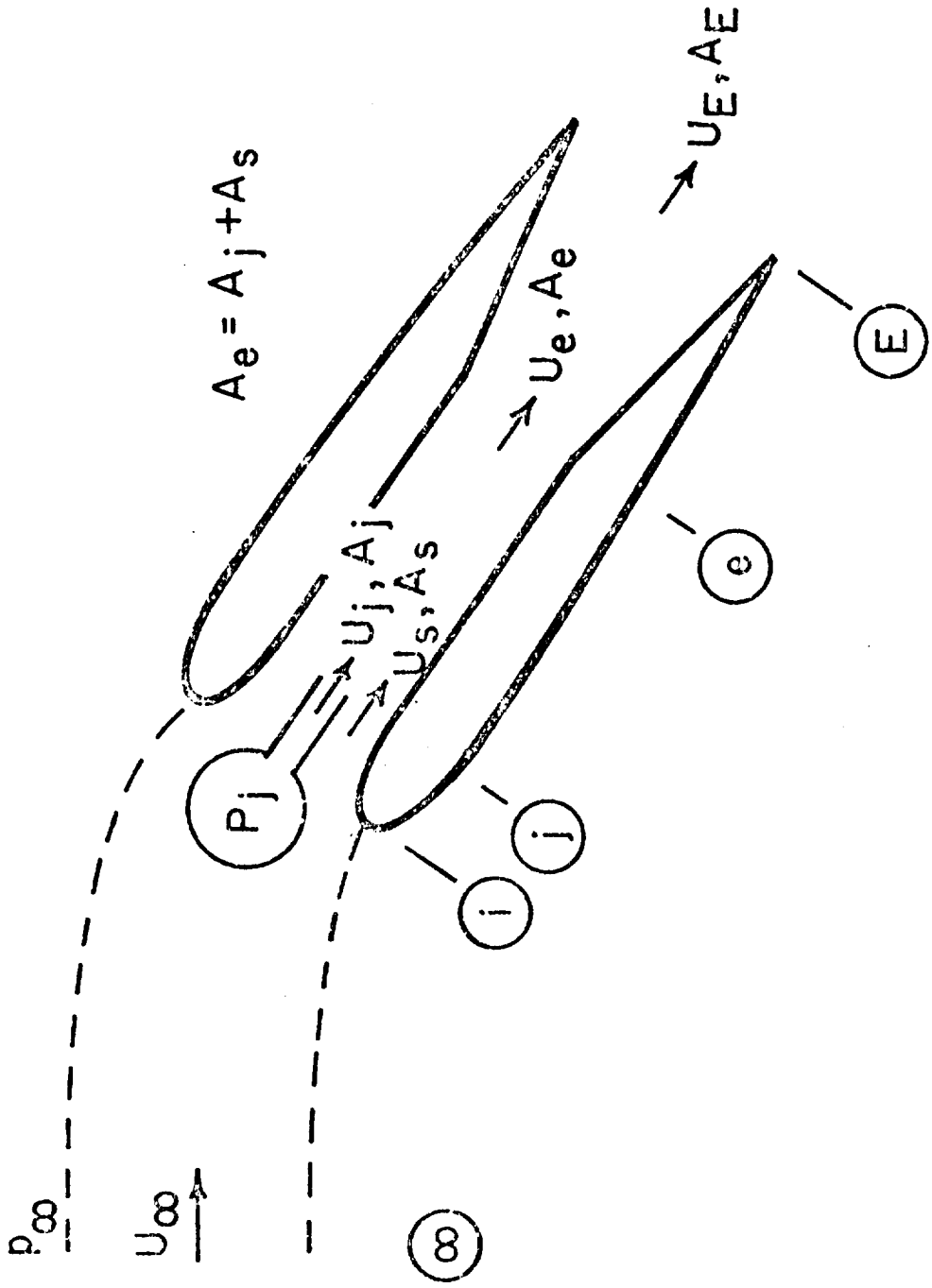

Figure 9.- Schematic representation of an ejector flap.

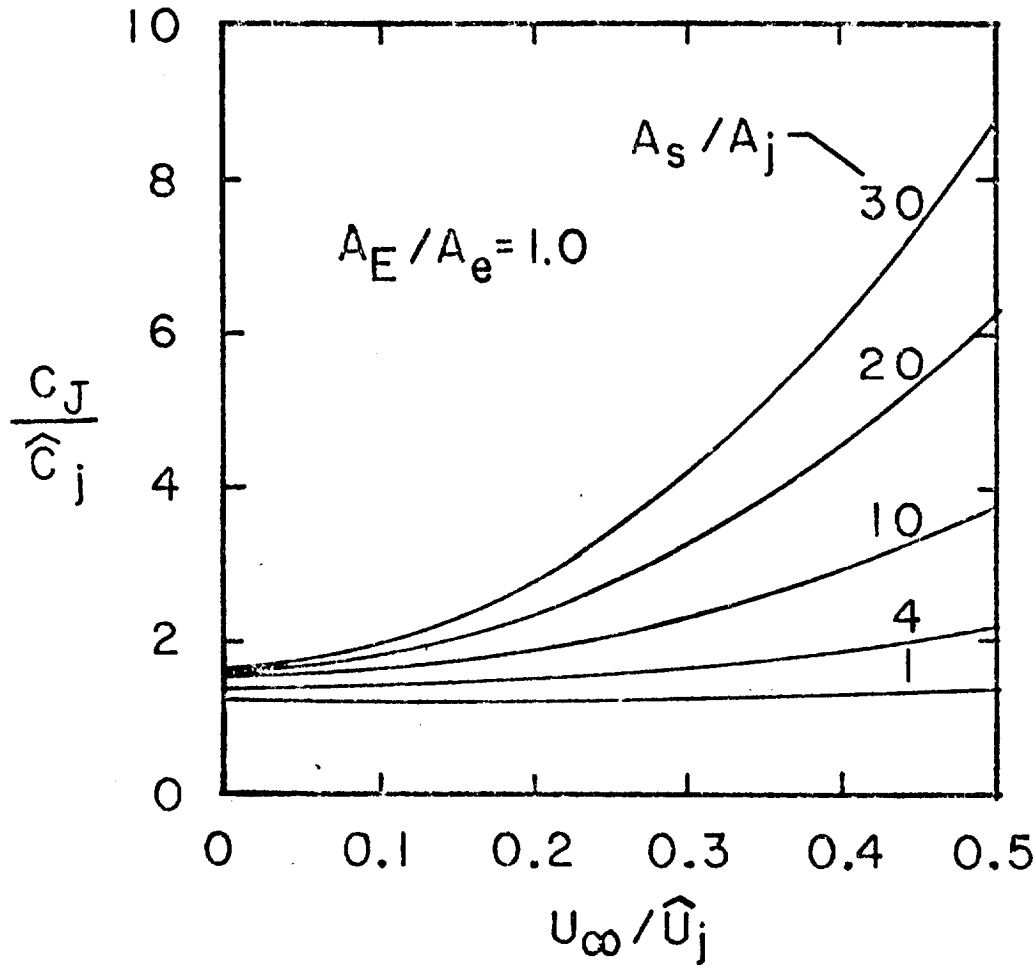

Figure 10.- Exit-momentum augmentation ratio as a function of the forward-speed ratio and injection-area ratio.

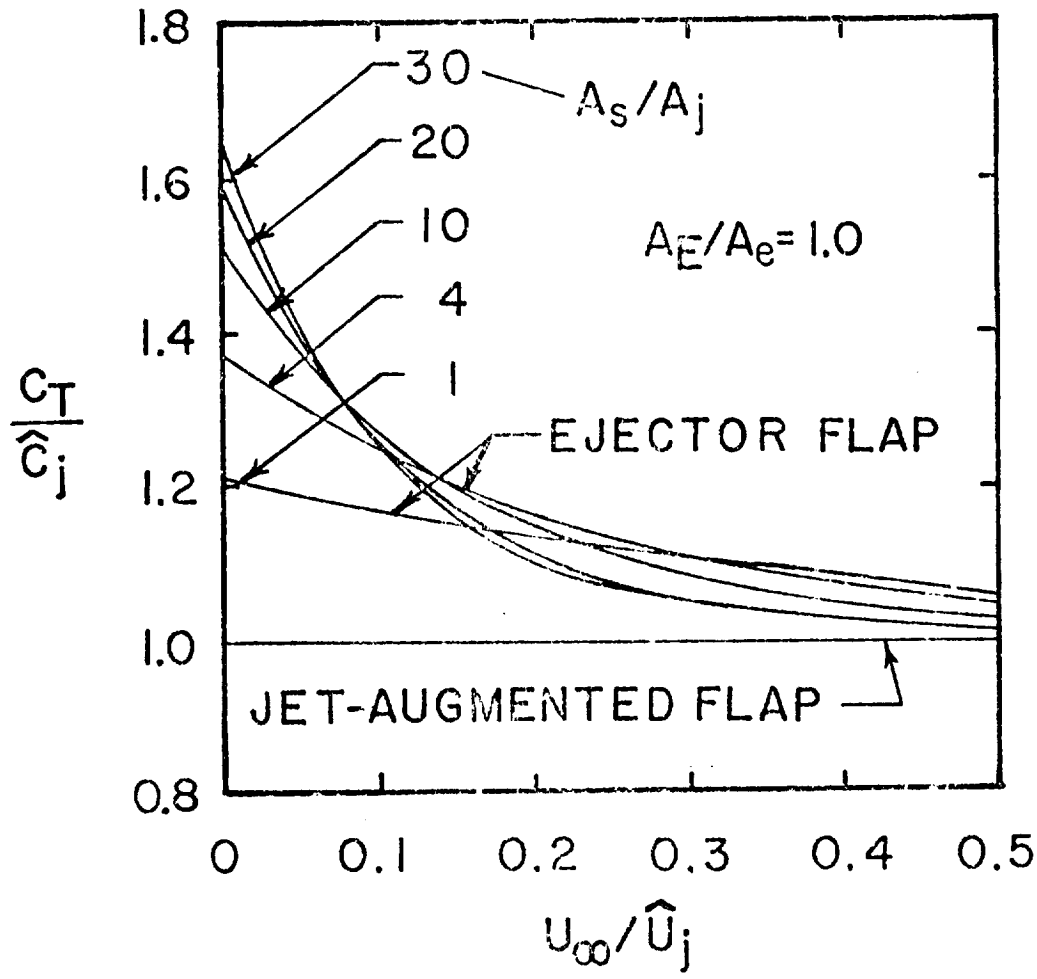

Figure 11.- Thrust-augmentation ratio as a function of the forward-speed ratio and injection-area ratio.

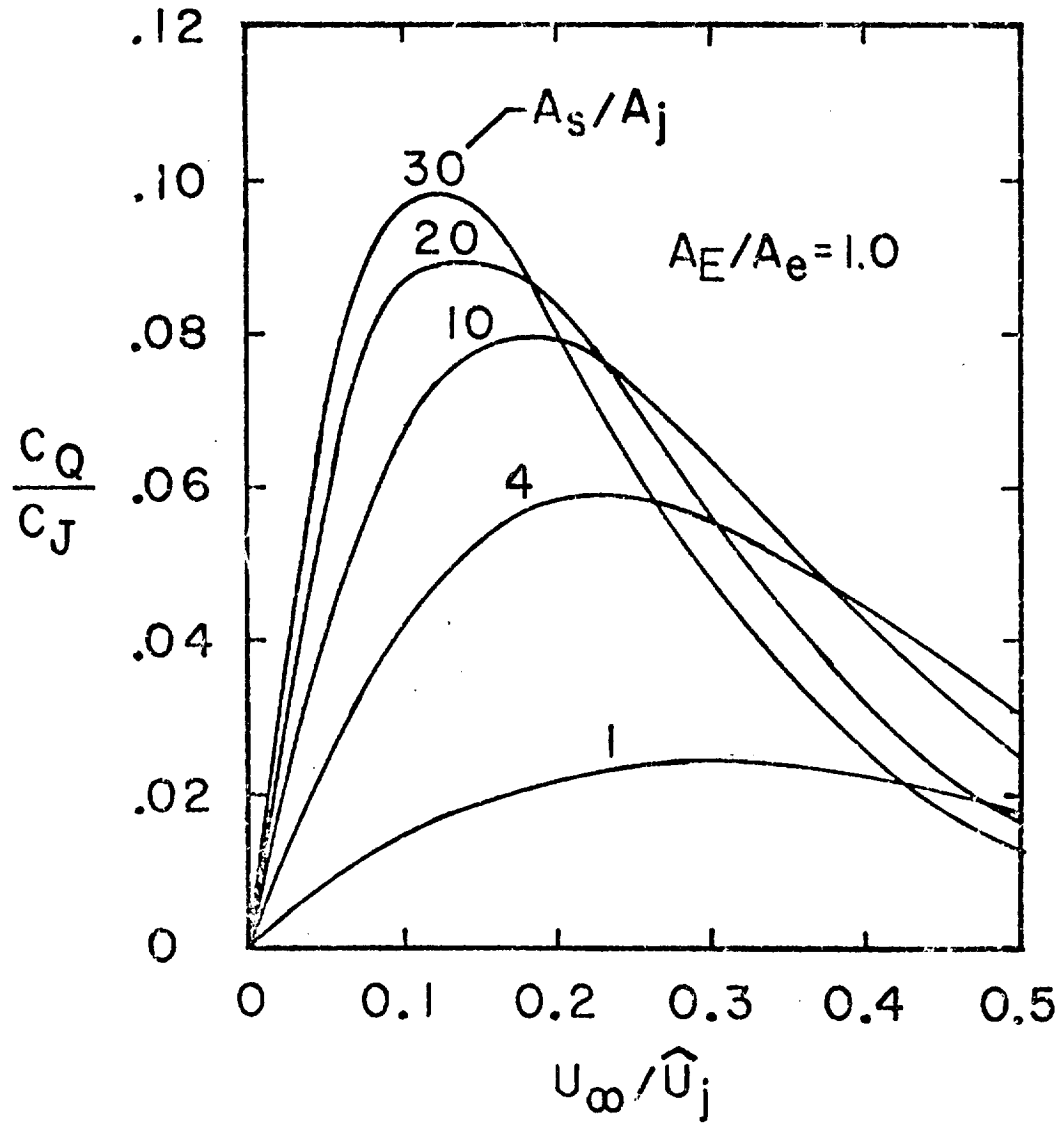

Figure 12.- Ratio of net suction coefficient to jet-momentum coefficient as a function of the forward-speed ratio and the injection-area ratio.

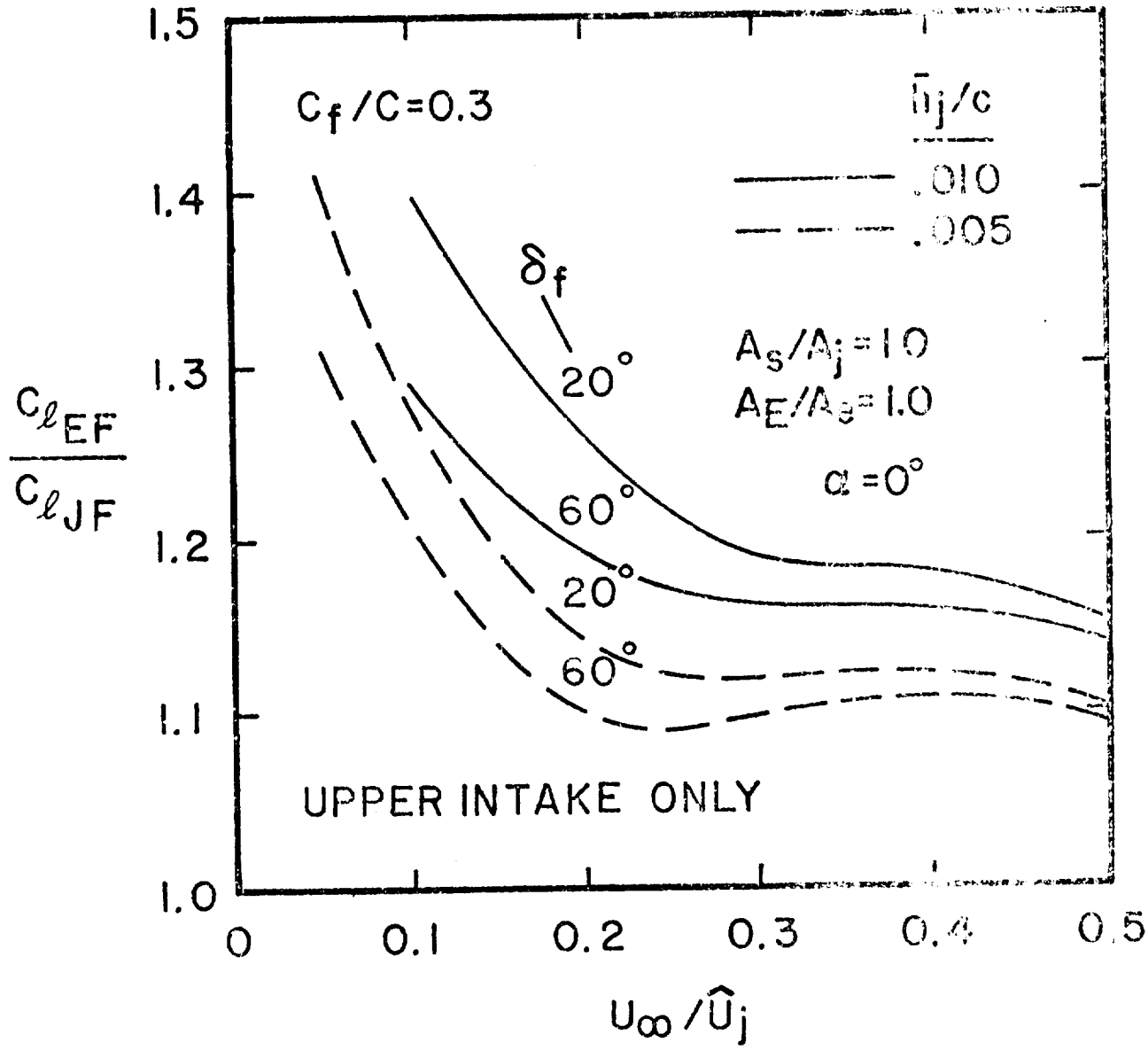

Figure 13.- Relative lift performance of ejector-flapped and jet-augmented-flapped wings.

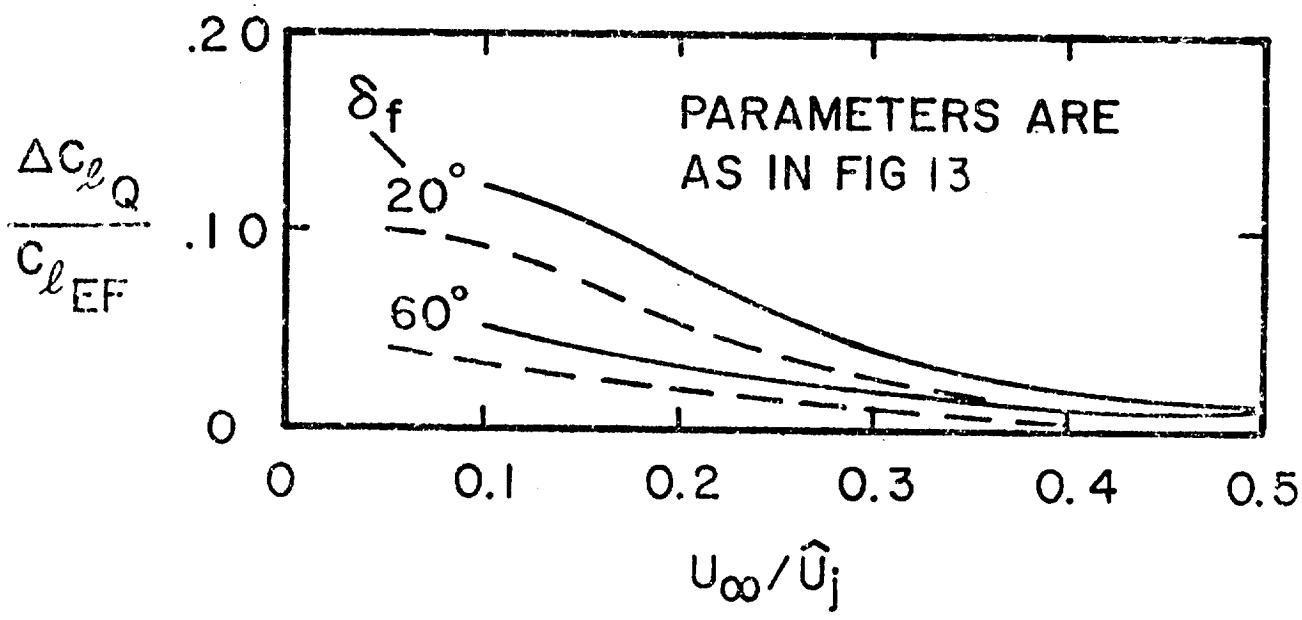

Figure 14.- Suction contribution to the lift of ejector-flapped wings.